



HAL
open science

Propagation of modeling uncertainty by polynomial chaos expansion in multidisciplinary analysis

S Dubreuil, Nathalie Bartoli, Christian Gogu, T Lefebvre

► **To cite this version:**

S Dubreuil, Nathalie Bartoli, Christian Gogu, T Lefebvre. Propagation of modeling uncertainty by polynomial chaos expansion in multidisciplinary analysis. *Journal of Mechanical Design*, 2016, 10.1115/1.4034110 . hal-01342356

HAL Id: hal-01342356

<https://hal.science/hal-01342356>

Submitted on 19 Jul 2016

HAL is a multi-disciplinary open access archive for the deposit and dissemination of scientific research documents, whether they are published or not. The documents may come from teaching and research institutions in France or abroad, or from public or private research centers.

L'archive ouverte pluridisciplinaire **HAL**, est destinée au dépôt et à la diffusion de documents scientifiques de niveau recherche, publiés ou non, émanant des établissements d'enseignement et de recherche français ou étrangers, des laboratoires publics ou privés.

Propagation of modeling uncertainty by polynomial chaos expansion in multidisciplinary analysis

S. Dubreuil

Onera - The French Aerospace Lab, F-31055 Toulouse France,
Email: sylvain.dubreuil@onera.fr

N. Bartoli

Onera - The French Aerospace Lab, F-31055 Toulouse France

C. Gogu

Université de Toulouse ; UPS, INSA, Mines Albi, ISAE ; ICA (Institut Clément Ader) ;
3 rue Caroline Aigle, F-31400 Toulouse, France

T. Lefebvre

Onera - The French Aerospace Lab, F-31055 Toulouse France

Multidisciplinary analysis (MDA) is nowadays a powerful tool for analysis and optimization of complex systems. The present study is interested in the case where MDA involves feedback loops between disciplines (i.e. the output of a discipline is the input of another and vice-versa). When the models for each discipline involve non-negligible modeling uncertainties, it is important to be able to efficiently propagate these uncertainties to the outputs of the MDA. The present study introduces a polynomial chaos expansion (PCE) based approach to propagate modeling uncertainties in MDA. It is assumed that the response of each disciplinary solver is affected by an uncertainty modeled by a random field over the design and coupling variables space. A semi intrusiv PCE formulation of the problem is proposed to solve the corresponding nonlinear stochastic system. Application of the proposed method emphasizes an important particular case in which each disciplinary solver is replaced by a surrogate model (e.g. kriging). Three application problems are treated, which show that the proposed approach can approximate arbitrary (non Gaussian) distributions very well at significantly reduced computational cost.

Nomenclature

x Lower case letter denoted deterministic variables (scalar or vector).

X Upper case letter denoted random variables (scalar or vector).

$x^{(k_0)}$ An exponent in parenthesis is used to set the value of the variable, i.e. $x^{(k_0)}$ is a given value of the deterministic variable x .

1 Introduction

This article addresses the topic of multidisciplinary analyses that can appear in the design of complex systems (e.g. aircraft), involving multiple interacting disciplines (e.g. aerodynamics, structural mechanics, propulsion for aircraft design). In the last decades, several authors have shown that taking into account interactions between disciplines in the design optimization process allows to reach a better design (with respect to a global criterion such as the range or fuel consumption), than the one obtained by sequential optimization [1]. Consequently several multidisciplinary optimization (MDO) strategies have been proposed (see [2] for a review). The most straightforward one is probably the multidisciplinary feasible (MDF) approach. It consists in a coupled multidisciplinary analysis (MDA), at each candidate design, during the optimization process. From a computational point of view, this coupled approach can be quite challenging, especially if iterative analysis between disciplines are necessary to reach compatibility conditions (as an example,

the equilibrium between the static deflection and the aerodynamics efforts applied on a wing). These types of interactions, sometimes called feedback or bidirectional loops [3] are of interest in the present paper.

The models used in the multidisciplinary analysis typically involve various levels of modeling errors, which induces a modeling uncertainty on the output of the model. Let us emphasize that these modeling uncertainties may not be constant with respect to the design variables and the coupling variables, but may vary over the design domain, since the model may be more accurate in some areas and less in others. Propagation of these modeling uncertainties through the design process must be carried out in order to quantify the resulting uncertainty on the objective function [4]. Indeed, relying only on the mean predicted values can lead to erroneous conclusions about the optimal design. Moreover, many studies prove the interest of taking into account objective function uncertainty in an optimization process ([5] for a well known example).

Among the various ways of modeling uncertainties into a numerical model, the probabilistic framework is the most common one and will also be used in this paper. This leads to the construction of the uncertainty MDO (UMDO) formulations. As for deterministic MDO formulations, coupled and uncoupled approaches are proposed. Examples of uncoupled approaches can be found in [6], [7], but this paper is focused on coupled approaches involving feedback loops. Moreover, let us note that, in the context of MDA, the probabilistic framework has been mainly used up to now to deal with uncertain model input parameters and not model uncertainties. For example in [8], [9] and [10] Monte Carlo Simulation (MCS) is used for propagating parameter uncertainties to the objective function. Concerning variable model uncertainties, *i.e* random fields with respect to the design and coupling variables, to the best of our knowledge, only [3] proposes a method to handle them in an MDA context. Their work is an adaptation of [7] in which a semi-uncoupled likelihood based simulation approach is proposed.

In order to solve the problem of model uncertainty propagation through the coupled MDA, we propose in this paper an approach based on the use of polynomial chaos expansion (PCE). The developed method constitutes an original application of classical PCE in an MDA context and we will discuss the advantages and drawbacks of this formulation compared to MCS. We will illustrate two real-case application problems in the context of preliminary aircraft design. The first one deals with regression models constructed from a historical database of aircraft parameters and performances. Such models involve significant uncertainty that varies within the design space since the regression models are more accurate in certain areas of the design space than in others. The second one deals with models approximated by kriging metamodels [11]. Due to the nature of the kriging metamodel, the model uncertainty varies within the design space (the model being the most accurate in the vicinity of the points that served for its construction).

The rest of the paper is organized as follows. Section 2.2 presents the MDA formalism and introduces the probabilistic

framework used for model uncertainties. More precisely, it describes the modeling of uncertainties by random fields and focuses on two particular cases. In the first one, the random fields construction is based on expert judgment possibly in conjunction with the use of a database and linear regression methods. In this case a perfectly correlated assumption is made concerning the correlation of the random field. In the second one, simplified models are kriging meta-models that intrinsically represent model uncertainties by conditioned Gaussian random fields. Section 3 proposes the resolution of the stochastic coupled MDA by PCE. This section contains the original part of the paper by introducing a semi-intrusive PCE approach. Section 4 is devoted to numerical applications and comparisons with Monte Carlo reference results. Efficiency of the proposed method is demonstrated first on an academic example and then on two examples based on conceptual aircraft design.

2 Back ground on MDA under uncertainty

2.1 Representation of uncertainties

This article addresses the issue of uncertainty propagation through coupled multidisciplinary problems. In this context a distinction can be made between two major types of uncertainties: aleatory and epistemic uncertainty. Aleatory uncertainty is also known as stochastic uncertainty, irreducible uncertainty, inherent uncertainty, variability or type I uncertainty. It can stem from environmental stochasticity, inhomogeneity of materials, fluctuations in time, variation in space, heterogeneity or other intrinsic differences in the features of a system. Epistemic uncertainty on the other hand, sometimes called reducible uncertainty or type II uncertainty, stems from lack of knowledge. This kind of uncertainty is usually related to scientific ignorance, measurement uncertainty (e.g. sensor uncertainty), insufficient experimental data or data censoring, thus in general terms lack of knowledge. In particular epistemic uncertainty includes uncertainty related to numerical approximations and model uncertainty. While aleatory uncertainty is typically being modeled within a probabilistic framework, alternative frameworks have been developed for modeling epistemic uncertainty (e.g. interval analysis [12], fuzzy sets [13], evidence theory [14], possibility theory [15]). Much debate has taken place over the best way to represent model uncertainty and no consensus was reached [16].

In this work we limit ourselves to the propagation of modeling uncertainty. Note however that approaches have also been proposed for propagation of both aleatory and epistemic uncertainties [3]. Furthermore, in this work we consider the modeling uncertainty within a probabilistic framework. While there is no consensus on the best framework for modeling epistemic uncertainty, we chose a probabilistic framework due to its extensive use and strong theoretical background. In particular it allows to treat Gaussian processes which provide an intrinsic probabilistic model error and which is commonly used with expensive black-box type numerical models. The two application problems provided in section 4.3 illustrate two such cases in aircraft de-

sign where probabilistic frameworks have been used for representing modeling uncertainty.

2.2 Introduction of model uncertainties in MDA

A classical deterministic MDA problem, of n disciplines involving feedback loops, could be written as a system of n equations,

$$y_i(z, y_{c^{(i)}}) = f_i(z, y_{c^{(i)}}), \quad i = 1, \dots, n \quad (1)$$

where, z stands for the vector of design variables, $y_{c^{(i)}}$ is the vector of the coupling variables for the discipline i . $c^{(i)}$ is the set of indexes that identify the coupling variables *i.e.* $\#(c^{(i)}) \leq (n-1)$ and $i \notin c^{(i)}$. Finally, f_i is the solver of discipline i . Let us precise that: with the previously introduced notations, disciplines i and j are said to have a feedback loop if $i \in c^{(j)}$ and $j \in c^{(i)}$. In the following, it is assumed that Eqn. (1) contains at least one feedback coupling. Discipline solvers f_i , $i = 1, \dots, n$ are black boxes. Definition of f_i is unknown to the user (note that f_i could be linear or nonlinear with respect to the design and coupling variables). It should be noted that this assumption is relevant in a multidisciplinary context, in which the designer (who is not necessarily an expert of each domain) is only a user of the disciplinary tool f_i provided by an expert of the discipline. Solution of Eqn. (1) is the vector y of size n . As we assume feedback coupling, and that f_i , $i = 1, \dots, n$ are black boxes, this solution is computed by an iterative algorithm. In the following, existence of a unique solution for Eqn. (1) is assumed by physical considerations. Finally, this study is focused on multidisciplinary analysis, not optimization, the vector of design variables z is thus a constant. Consequently, the deterministic problem is: find y_i , $i = 1, \dots, n$ such that Eqn. (1) stands for an arbitrary $z = z^{(0)}$. Note that this leads us to leave aside the dependence in z in the rest of the paper.

Given this deterministic MDA formulation we now introduce modeling uncertainties that will affect each discipline. Accordingly we associate the modeling uncertainty ε_i to the solver f_i such that, $y_i^*(y_{c^{(i)}}) = f_i(y_{c^{(i)}}) + \varepsilon_i(y_{c^{(i)}})$ where y_i^* is a reference value (either obtained by experimental set up or high fidelity numerical model). It should be noted that, the modeling uncertainty depends on the coupling variables (it also depends on the design variables z , we recall that z is a constant in this study). An exhaustive presentation of methods for quantification of modeling uncertainties is out of the scope of this study, but we refer the interested reader to [17]. In the present work, a probabilistic modeling of these uncertainties has been chosen. In the numerical examples presented in section 4 the model uncertainty quantification will be obtained either by prediction variance formulations associated with regression methods on experimental databases or by the use of kriging surrogate models, which explicitly contains an uncertainty model in its formulation. We introduce S_i the space of the coupling variables $y_{c^{(i)}}$ (it is assumed that $S_i \subset \mathbb{R}^{\#c^{(i)}}$) and a probability space (Ω, F, P) where Ω is the space of elementary events with elements ω , F is a

σ -algebra on Ω and P a probability measure on F . Then, $\varepsilon_i(y_{c^{(i)}}, \omega)$ is modeled as a real valued continuous random field on S_i (*i.e.* $\forall y_{c^{(i)}}^{(k_0)} \in S_i$, $\varepsilon_i(y_{c^{(i)}}^{(k_0)}, \omega)$ is a real valued random variable). It is assumed that $\varepsilon_i(y_{c^{(i)}}, \omega)$, $i = 1, \dots, n$ are independent random fields. Concerning the choice of the covariance function of the random field $\varepsilon_i(y_{c^{(i)}}, \omega)$, two particular cases will be studied:

1. Perfectly correlated random field.

$\forall (y_{c^{(i)}}^{(k_1)}, y_{c^{(i)}}^{(k_2)}) \in S_i^2$, the random variables $\varepsilon_i(y_{c^{(i)}}^{(k_1)}, \omega)$ and $\varepsilon_i(y_{c^{(i)}}^{(k_2)}, \omega)$ are perfectly dependent *i.e.* $\varepsilon_i(y_{c^{(i)}}^{(k_1)}, \omega) = g(\varepsilon_i(y_{c^{(i)}}^{(k_2)}, \omega), y_{c^{(i)}}^{(k_1)})$, where g is a deterministic function. In the following this case will be denoted by *perfectly correlated* case.

2. $\varepsilon_i(y_{c^{(i)}}, \omega)$ is a Gaussian random field conditioned on some design of experiments (DOE) with a specified covariance kernel. This case corresponds to the one where a kriging meta-model is used as a simplified model and so it will be denoted as *kriging* case.

We introduce the stochastic version of Eqn. (1) by taking into account the modeling uncertainty,

$$Y_i(\omega) = f_i(Y_{c^{(i)}}(\omega)) + \varepsilon_i(Y_{c^{(i)}}(\omega), \omega), \quad i = 1, \dots, n \quad (2)$$

where Y_i , $i = 1, \dots, n$ are real valued random variables. The solution of the system of Eqn. (2) is the joint probability distribution of the random vector Y_i , $i = 1, \dots, n$. One should note that the difficulty in solving Eqn. (2) is due to the presence of the coupling random variables $Y_{c^{(i)}}(\omega)$. Resolution of Eqn. (2) involves the discretization of the random fields $\varepsilon_i(y_{c^{(i)}}, \omega)$, $i = 1, \dots, n$. In the *perfectly correlated* case this discretization is achieved by a single random variable. In the *kriging* case we classically rely on the Karhunen-Loève (KL) decomposition.

Resolution of Eqn. (2) can be achieved by Monte Carlo simulation (MCS), which basically consists in solving N_{MCS} deterministic systems (Eqn. (2) with N_{MCS} constant values for ω). Usually, MCS could be unaffordable if one evaluation of the discipline solvers, f_i , $i = 1, \dots, n$ is time consuming. Moreover, the MCS results is a collection of response realizations from which one can estimate statistics with an accuracy depending on the number of simulations. Dealing with this representation of the response might have some drawbacks for post processing.

To deal with these two shortcomings polynomial chaos expansion (PCE) offers some advantages by providing a functional representation of the response Y_i , $i = 1, \dots, n$ with respect to the random inputs. Besides computational cost savings, a functional representation allows an easy access to relevant post processing information such as global sensitivity analysis (GSA see [18]).

3 Uncertainty propagation by polynomial chaos expansion

3.1 Perfectly correlated case

First of all, we parametrize the problem with a vector of n independent standard normal variables called $\xi : (\Omega, F) \rightarrow (\mathbb{R}^n, \mathcal{B}_n)$. Then, Eqn. (2) can be rewritten,

$$Y_i(\xi) = f_i(Y_{c(i)}(\xi)) + \varepsilon_i(Y_{c(i)}(\xi), \xi_i), \quad i = 1, \dots, n \quad (3)$$

where the dependence in ω is omitted for sake of clarity.

We now introduced the Hermite PCE ([19]) of a given discipline i . Suppose that $E[Y_i^2] < \infty$, then $Y_i(\xi)$ reads,

$$Y_i(\xi) = \sum_{j=0}^{\infty} a_j^{(Y_i)} \Psi_j(\xi) \quad (4)$$

where $a_j^{(Y_i)}$ denoted the unknown coefficients of Y_i PCE and $\{\Psi_j\}_{j=0}^{P-1}$ are the n -variate Hermite polynomials. It should be noted that the choice of Hermite PCE is motivated for the sake of simplicity, but the use of more advanced PCE methods is also possible (e.g. [20] and [21] for generalized PCE, [22] for iterative generalized PCE and [23] for multi elements generalized PCE).

Decomposition Eqn. (4) is truncated to P terms such that,

$$Y_i(\xi) \approx \hat{Y}_i(\xi) = \sum_{j=0}^{P-1} a_j^{(\hat{Y}_i)} \Psi_j(\xi). \quad (5)$$

The retained truncation strategy consists in keeping all the polynomials with a degree less or equal to d , hence $P = \frac{(n+d)!}{n!d!}$. Approximation $\hat{Y}_i(\xi)$ leads to the definition of the residual r_i corresponding to the introduction of the PCE approximation (Eqn. (5)) in the line i of Eqn. (3)),

$$r_i = \hat{Y}_i(\xi) - f_i(\hat{Y}_{c(i)}(\xi)) - \varepsilon_i(\hat{Y}_{c(i)}(\xi), \xi_i). \quad (6)$$

We now seek to determine the coefficients $a_j^{(\hat{Y}_i)}$ of Eqn. (5). For this purpose a non intrusive projection approach is used (let us recall that the solver f_i is only accessible as a black box function). It consists in imposing the projection of the residual r_i on the vectors $\{\Psi_j\}_{j=0}^{P-1}$ to be zero, i.e $E[r_i \Psi_j] = 0$, $j = 0, \dots, P-1$ leading to

$$a_j^{(\hat{Y}_i)} E[\Psi_j^2] = \int_{\mathbb{R}^n} (f_i(\hat{Y}_{c(i)}(\xi)) + \varepsilon_i(\hat{Y}_{c(i)}(\xi), \xi_i)) \Psi_j(\xi) \varphi(\xi) d\xi \quad (7)$$

where φ is the probability density function of a normal standard random variable. In practice, the integral in Eqn. (7) is computed by Gauss quadrature, leading to (assuming a num-

ber Q of quadrature nodes)

$$a_j^{(\hat{Y}_i)} E[\Psi_j^2] \approx \sum_{q=1}^Q w^{(q)} \left[\left(f_i(\hat{Y}_{c(i)}(\xi^{(q)})) + \varepsilon_i(\hat{Y}_{c(i)}(\xi^{(q)}), \xi_i^{(q)}) \right) \Psi_j(\xi^{(q)}) \right] \quad (8)$$

where $w^{(q)}$ denotes the quadrature weight associated to the node $\xi^{(q)}$. The term $f_i(\hat{Y}_{c(i)}(\xi^{(q)}))$ is computed by the solver f_i and the term $\varepsilon_i(\hat{Y}_{c(i)}(\xi^{(q)}), \xi_i^{(q)})$ is evaluated by the isoprobabilistic transformation,

$$\begin{aligned} \Phi(\xi_i^{(q)}) &= F_{\varepsilon_i(\hat{Y}_{c(i)}(\xi^{(q)}), \xi_i)}(\varepsilon_i(\hat{Y}_{c(i)}(\xi^{(q)}), \xi_i^{(q)})) \\ \Rightarrow \varepsilon_i(\hat{Y}_{c(i)}(\xi^{(q)}), \xi_i^{(q)}) &= F_{\varepsilon_i(\hat{Y}_{c(i)}(\xi^{(q)}), \xi_i)}^{-1}(\Phi(\xi_i^{(q)})). \end{aligned}$$

Let us specify that, in the cases studied in this article, $\varepsilon_i(\hat{Y}_{c(i)}(\xi^{(q)}), \xi_i)$, $i = 1, \dots, n$ are always independent, with *classical* probability distributions (normal, uniform etc.) which makes the computation of $F_{\varepsilon_i(\hat{Y}_{c(i)}(\xi^{(q)}), \xi_i)}^{-1}$ straightforward. For other cases one can refer to [24] and [25] for a detailed presentation of generalized isoprobabilistic transformations.

After having introduced the PCE for each discipline, we now come back to the system of n equation of Eqn. (3), by approximating each line of the system by its PCE (as in Eqn. (5)), such as to obtain the nonlinear system,

$$\begin{aligned} \hat{Y}_i(\xi) &= \sum_{j=0}^{P-1} a_j^{(\hat{Y}_i)} \Psi_j(\xi) \\ &= f_i(\hat{Y}_{c(i)}(\xi)) + \varepsilon_i(\hat{Y}_{c(i)}(\xi), \xi_i), \quad i = 1, \dots, n \end{aligned} \quad (9)$$

where the unknowns are the coefficients $a_j^{(\hat{Y}_i)}$, $i = 1, \dots, n$, $j = 0, \dots, P-1$. This nonlinear system is solved by a fixed point algorithm described in Algo. 1. This choice is motivated by the simplicity of implementation especially for updating the probability distribution of the random variable $\varepsilon_i(\hat{Y}_{c(i)}(\xi^{(q)}), \xi_i)$ at each iteration. Note that we call $a_{j,0}^{(\hat{Y}_i)}$, $i = 1, \dots, n$, $j = 0, \dots, P-1$ the initial PCE coefficients or the coefficients of the previous iteration and $a_{j,1}^{(\hat{Y}_i)}$, $i = 1, \dots, n$, $j = 0, \dots, P-1$ the coefficients at the current iteration. Let $\hat{Y}_{i,0}$ and $\hat{Y}_{i,1}$ represent respectively the PCE approximation given by Eqn. (5) computed with coefficients $a_{j,0}^{(\hat{Y}_i)}$ and $a_{j,1}^{(\hat{Y}_i)}$, $i = 1, \dots, n$, $j = 0, \dots, P-1$. The algorithm is considered converged when the difference between the coefficients of the previous and current iteration is below a certain threshold. More precisely the stopping criterion is the relative variation of the response, at each quadrature nodes, between two iterations. This criterion is retained as it can be used, with the same threshold value err_0 for MCS, which allows a meaningful comparison between the two approaches. Finally, it should be noted that the convergence of Algo. 1 will be discussed in several numerical examples in section 4.

```

Initialize  $a_{j,0}^{(\hat{Y}_i)}$ ,  $i = 1, \dots, n$ ,  $j = 0, \dots, P-1$ 
while #  $\left\{ l/err(\xi^{(q)}) \geq err_0, q = 1, \dots, Q \right\} > 1$  do
   $err(\xi^{(q)}) = 0$ ,  $q = 1, \dots, Q$ 
  for  $i = 1, \dots, n$  do
    for  $\alpha \in c^{(i)}$  do
      Compute  $\hat{Y}_\alpha(\xi^{(q)})$  by Eqn. (5) and
      coefficients  $a_{j,0}^{(\hat{Y}_\alpha)}$ 
    end
    Update the probability distribution of
     $\varepsilon_i(\hat{Y}_{c^{(i)}}(\xi^{(q)}), \xi_i)$ 
    for  $j = 0, \dots, P-1$  do
      Compute  $a_{j,1}^{(\hat{Y}_i)}$  by Eqn. (8)
    end
    Compute  $err_i(\xi^{(q)}) = \left| \frac{\hat{Y}_{i,0}(\xi^{(q)}) - \hat{Y}_{i,1}(\xi^{(q)})}{\hat{Y}_{i,0}(\xi^{(q)})} \right|$ ,
     $q = 1, \dots, Q$ 
     $err(\xi^{(q)}) = err(\xi^{(q)}) + err_i(\xi^{(q)})$ ,
     $q = 1, \dots, Q$ 
    Set  $a_{j,0}^{(\hat{Y}_i)} = a_{j,1}^{(\hat{Y}_i)}$ ,  $j = 0, \dots, P-1$ 
  end
end

```

Algorithm 1: Fixed point algorithm used to solve Eqn. (9)

3.2 Kriging case

We are now interested in the case where the models Y_i are provided by kriging metamodels.

Kriging has been introduced by [26] in the geostatistics field. As the focus of the present article is not on the kriging method, only the necessary background is explained. Literature on Kriging is wide and readers could refer, for example, to [27] for a detailed presentation.

Let us call $y_i^*(y_{c^{(i)}})$ the *actual* unknown response. Kriging modeling assumes that $y_i^*(y_{c^{(i)}})$ is a realization of a Gaussian process (GP), denoted by $H_i(y_{c^{(i)}})$ with mean $\mu_i(y_{c^{(i)}})$ and covariance function $C_i(y_{c^{(i)}}^{(k_1)}, y_{c^{(i)}}^{(k_2)})$. Then, assuming that $y_i^*(y_{c^{(i)}})$ is known on a given DOE of size s , kriging consists in the construction of a conditioned GP, denoted by Y_i of mean $f_{i,s}(y_{c^{(i)}})$ and covariance function $k_{i,s}(y_{c^{(i)}}^{(k_1)}, y_{c^{(i)}}^{(k_2)})$ where $(y_{c^{(i)}}^{(k_1)}, y_{c^{(i)}}^{(k_2)}) \in S_i^2$. Expressions of $f_{i,s}(y_{c^{(i)}})$ and $k_{i,s}(y_{c^{(i)}}^{(k_1)}, y_{c^{(i)}}^{(k_2)})$ in terms of $\mu_i(y_{c^{(i)}})$ and $C_i(y_{c^{(i)}}^{(k_1)}, y_{c^{(i)}}^{(k_2)})$ can be found in [27].

In the context of the stochastic system of Eqn. (2), Y_i is a GP with a random mean $f_{i,s}(Y_{c^{(i)}})$ and a random covariance function $k_{i,s}(Y_{c^{(i)}}^{(k_1)}, Y_{c^{(i)}}^{(k_2)})$. We introduce now the KL decomposition [19] of Y_i .

$$Y_i(Y_{c^{(i)}}(\omega), \omega) = f_{i,s}(Y_{c^{(i)}}(\omega)) + \sum_{m_i=1}^{\infty} \sqrt{\lambda_{m_i}} V_{m_i}(Y_{c^{(i)}}(\omega)) \xi_{m_i}(\omega) \quad (10)$$

In the particular case of GP, ξ_{m_i} are independent standard normal random variables. λ_{m_i} and V_{m_i} are respectively the eigenvalues and corresponding eigenvectors of the covari-

ance function $k_{i,s}(y_{c^{(i)}}^{(k_1)}, y_{c^{(i)}}^{(k_2)})$. In practice, the KL decomposition (Eqn. (10)) is truncated to M_i terms (corresponding to the M_i largest eigenvalues). λ_{m_i} and V_{m_i} are found as solutions of the equation,

$$\int_D k_{i,s}(x_1, x_2) V_{m_i}(x_2) dx_2 = \lambda_{m_i} V_{m_i}(x_1). \quad (11)$$

The solution of this equation is discussed in [19]. Except for special covariance functions, solutions of Eqn. (11) must be computed numerically (see [19] for details). In the rest of the paper, the discretization of the domain D on a fine regular grid is used.

By analogy with the previous section, we introduce a vector ξ of M independent standard normal random variables ($M = \sum_{i=1}^n M_i$) and $\{\Psi_j\}_{j=0}^{\infty}$ the Hermite polynomials of M variables. Then, one can compute the truncated PCE of Y_i on this basis. To this purpose, coefficients $a_j^{(\hat{Y}_i)}$, $j = 0, \dots, P-1$ are still obtained by a non intrusive projection approach, leading to

$$a_j^{(\hat{Y}_i)} E[\Psi_j^2] = \int_{\mathbb{R}^M} \left(f_{i,s}(\hat{Y}_{c^{(i)}}(\xi)) + \sum_{m_i=1}^{M_i} \sqrt{\lambda_{m_i}} V_{m_i}(Y_{c^{(i)}}(\xi)) \xi_{m_i} \right) \Psi_j(\xi) \varphi(\xi) d\xi \quad (12)$$

which is, once again, computed by Gauss quadrature.

The corresponding nonlinear system, resulting from the introduction of the KL expansion into Eqn. (2), is solved by Algo. 1.

3.3 Remarks

The first remark concerns the random fields $\varepsilon_i(y_{c^{(i)}})$, $i = 1, \dots, n$. In the following it is assumed that these random fields respect the physics of the problem and that for all $\omega^{(0)} \in \Omega$, there exists a unique solution for Eqn. (2). It should be noted that, in practice, guarantying this assumption *a priori* is not straightforward, in particular for the *kriging* case. Nevertheless, in section 4 this assumption is experimentally verified during MCS.

The second remark about the methods introduced in the previous sections concerns the stochastic dimension of the problems. In the *perfectly correlated* case the stochastic dimension is equal to the number of disciplines n , whereas in the *kriging* case this dimension is equal to $M = \sum_{i=1}^n M_i$ (which is between $2n$ and $6n$ for the problem we tested). After this remark, let us introduce a *simplified kriging* case, which is the *perfectly correlated* case assuming that $\varepsilon_i(Y_{c^{(i)}}(\xi^{(q)}), \xi_i)$ is a Gaussian random variable of zero mean and variance given by the kriging model. Roughly speaking this leads to replace the covariance of the kriging by a perfect correlation assumption. Then, it is interesting to identify the situations for which this *simplified kriging* case is a correct approximation of the *kriging* case. Indeed, it allows to significantly reduce the stochastic dimension. Intuitively, one is interested in the values of the correlation functions of the

kriging surrogate models in the vicinity of the solution of Eqn. (2). Numerical experiments are presented in section 4 to illustrate this idea.

4 Numerical applications

4.1 Monte Carlo reference and approximation by PCE

The solution of Eqn. (2) is the joint probability distribution of Y_i , $i = 1, \dots, n$. In the following numerical examples, this probability distribution cannot be calculated analytically and will be estimated by MCS. For each MCS simulation the corresponding deterministic system (Eqn. (2) with a constant ω value) is solved by the fixed point algorithm. The same starting point is used for MCS and for the initialization step of Algo. 1. Finally, for the *kriging* case, the same KL decomposition is used for MCS and PCE approaches.

In order to quantify the accuracy of the method the following procedure is proposed. We call $\hat{F}_{MCS}(y)$ the empirical joint CDF of the random vector Y_i , $i = 1, \dots, n$ estimated by MCS. We also denote by $\hat{F}_{PCE}(y)$ the empirical joint CDF of the random vector \hat{Y}_i , $i = 1, \dots, n$ (where \hat{Y}_i is the PCE approximation of Y_i). We now introduce the following estimator of the mean relative error between these two empirical CDF defined by,

$$Err^{(Y_i, i=1, \dots, n)} = \frac{1}{N_{grid}} \sum_{k=1}^{N_{grid}} \left| \frac{\hat{F}_{MCS}(y^{(k)}) - \hat{F}_{PCE}(y^{(k)})}{\hat{F}_{MCS}(y^{(k)})} \right| \quad (13)$$

where N_{grid} is the number of estimation points $y^{(k)} \in \mathbb{R}^n$. These estimation points are located on a DOE over the variation domain of Y_i , $i = 1, \dots, n$. The sampling size for the MCS procedures is set to 100000 and, in practice, only the points $y^{(k)}$ such that $\hat{F}_{MCS}(y^{(k)}) \in [0.01, 0.99]$ will be considered for the computation of Err . It is then reasonable to assume that the sampling variability of Err is almost zero. Note that this procedure is coherent with the proposed method, in that the proposed approach aims at approximating the global behavior of the true probability distribution (without any focus on probability tails for which dedicated methods are available). Moreover, we highlight the fact that the PCE approach is purely deterministic and that the sampling variability of estimator Err is only due to MCS procedures and that this variability can be driven to zero by choosing a large sample size.

Finally let us specify that in all the following examples, the construction of Hermite polynomials and the associate quadrature rules rely on the python package OpenTURNS¹. Construction of the kriging models is done with the python package scikit learn [28] with a constant trend and a square exponential covariance kernel. Stopping criterion err_0 for Algo 1 and MCS is set to $err_0 = 10^{-7}$.

Table 1. Convergence of Algo. 1 with respect to the degree of the PCE approximation. P is the size of the polynomial basis and Q the number of quadrature points.

d	P	Nb unknowns	Q	N_{iter} Algo. 1	$N_{eval} f_i$
2	6	12	36	7	252
3	10	20	49	7	343
4	15	30	64	8	512
5	21	42	81	8	648

4.2 Sellar test case

4.2.1 Description

This test case, inspired by [29], counts two disciplines and one objective function. According to the formalism used in this paper the deterministic problem reads,

$$\begin{aligned} y_1 &= z_1^2 + z_2 - 0.2y_2 \\ y_2 &= \sqrt{y_1} + z_1 + z_2 \\ y_3 &= z_2 + y_1 + e^{-y_2} \end{aligned} \quad (14)$$

This system contains one feedback loop between y_1 and y_2 . The objective function is y_3 . Design variables z_1 and z_2 are constant such that $z_1 = 6$, $z_2 = 2$.

4.2.2 Perfectly correlated case: uniform random fields

For this first example it is assumed that disciplines y_1 and y_2 are affected by uniform random fields $\epsilon_1(y_2, \omega)$ and $\epsilon_2(y_1, \omega)$. Dependence of the uniform distributions parameters with respect to the coupling variables is arbitrarily chosen such as $\epsilon_1 \sim U(-0.2y_2, 0.2y_2)$ and $\epsilon_2 \sim U(-\sqrt{y_1}, \sqrt{y_1})$. It is also assumed that the model of the objective function y_3 is perfect, so, the stochastic dimension of the problem is $n = 2$. Figure 1 i) illustrates one realization of the random model and the bounds of the uniform random fields.

Reference results are obtained by MCS with $N_{MCS} = 100000$ simulations. Over these N_{MCS} simulations, the average number of iterations used to reach the convergence is $\mu_{MC} = 4.78$ with a coefficient of variation of 20%. The number of disciplinary solvers evaluations is approximately equal to $N_{MCS} \times \mu_{MC} = 478000$.

Objective of this example is to illustrate the convergence of the Algo. 1 with respect to the maximal degree d of the PCE. Quadrature level is chosen iteratively such that the relative differences between the coefficients $a_i^{(Y_3)}$ for two consecutive quadrature levels are all less than 5%. A full tensorization of the one dimensional quadrature rule is performed to obtain the quadrature rule in dimension n . Note that our objective here is not to optimize the quadrature level but to choose one that ensures a numerical integration error negligible compared to the truncation error. Table 1 gives the number of iterations of Algo. 1 for $d = 2$ to $d = 5$ to converge, the number Q of quadrature nodes used and the corresponding number of disciplinary solver evaluations. The first remark is that the number of iterations of the Algo. 1

¹<http://www.openturns.org/>

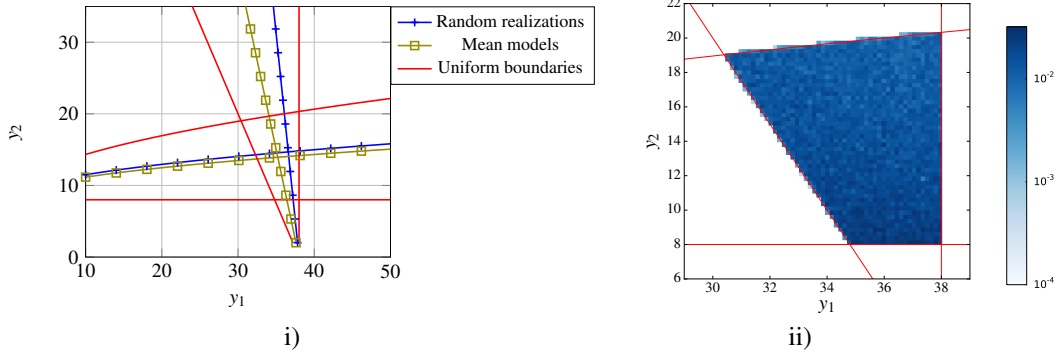


Fig. 1. i) Illustration of the sellar test case with uniform model uncertainties. In green the deterministic case, in blue a random realization and in red the boundaries of the uniform random fields ii) PDF of (Y_1, Y_2) , MCS results (100000 simulations)

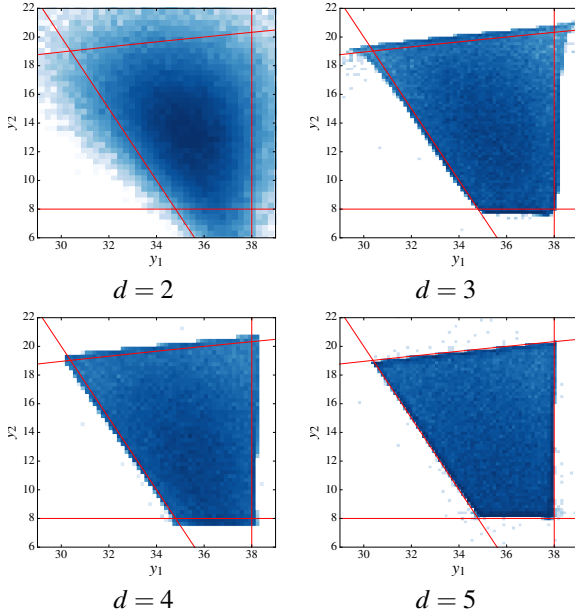


Fig. 2. PDF of \hat{Y}_1, \hat{Y}_2 obtained by PCE for degree $d = 2$ to $d = 5$. The same color scale as Fig. 1 ii) is used.

is almost insensitive to the number of unknown coefficients $a_j^{(Y_i)}$ (the number of unknown coefficients is equal to $P \times n$). Indeed, it only goes from 7 to 8 iterations while the number of unknown coefficients goes from 12 to 42. After this remark about the convergence of the Algo. 1, the accuracy of the approximation is now studied. First, a visual comparison is performed between the PDF of (Y_1, Y_2) obtained by MCS and by PCE. Figure 1 ii) presents the MCS reference results while Fig. 2 presents the results obtained by PCE approximation for $d = 2$ to $d = 5$. These figures (and all the followings in the numerical applications section) are normalized two dimensional histograms.

Figure 2 shows that the proposed PCE approach converges to the reference results with respect to the degree of the approximation. More precisely a correct approximation is obtained for $d = 4$. Finally, it is notable that for $d = 5$, even if the approximation is the best one according to the CDF error criterion defined by Eqn. (13) (see next paragraph), some

realizations stand far outside the uniform boundaries (one can note more isolated blue dots than for $d = 4$). This is due to the strong oscillations obtained with polynomials of high degree classically denoted by Gibbs phenomenon (see [30]). As the proposed approach is applied with Hermite PCE this behavior is expected. Nevertheless, more advanced PCE approaches cited previously may fix this issue.

The error criterion defined by Eqn. (13) with respect to the degree d of the PCE approximation for the estimation of the CDF of (Y_1, Y_2) is now evaluated. The domain $[30, 38] \times [8, 21]$ is discretized on a regular grid of $50 \times 50 = 2500$ points. Then, keeping only the points such that $\hat{F}_{MCS}(y^{(i)}) \in [0.01, 0.99]$ leads to $N_{grid} = 1536$. The results are, $Err_{d=2}^{(Y_1, Y_2)} \approx 15.80\%$, $Err_{d=3}^{(Y_1, Y_2)} \approx 6.95\%$, $Err_{d=4}^{(Y_1, Y_2)} \approx 6.72\%$, $Err_{d=5}^{(Y_1, Y_2)} \approx 3.05\%$. The same error criterion for the CDF of the objective function Y_3 is also evaluated. It is evaluated on the domain $[30, 45]$ discretized in 100 points. After the selection of the points such that $\hat{F}_{MCS}(y^{(i)}) \in [0.01, 0.99]$ one gets $N_{grid} = 90$, leading to $Err_{d=2}^{(Y_3)} \approx 10.33\%$, $Err_{d=3}^{(Y_3)} \approx 4.16\%$, $Err_{d=4}^{(Y_3)} \approx 3.89\%$, $Err_{d=5}^{(Y_3)} \approx 1.88\%$.

These results show that the relative errors tend toward zero with respect to the degree d of the PCE which is coherent with the theoretical results. We emphasize that despite the Gibbs phenomenon, the best results are obtained with the highest degree.

Finally, the proposed method is efficient on this first example with less than 650 disciplinary solver evaluations for the PCE approach (depending on the chosen degree, see Tab. 1) compared to 478000 evaluations for the MCS method.

4.2.3 Kriging case

In this section kriging metamodels are used as surrogate models of each disciplinary solver. In order to have an uncoupled approach, each kriging model is built on its own DOE. We denote by $Z_1 = [-10, 10]$, and $Z_2 = [0, 10]$ the intervals of variation of the design variables z_1 and z_2 , and by $S_1 = [0, 24]$ and $S_2 = [3.16, 100]$ the intervals of variation of $y_{c(1)} = y_2$ and $y_{c(2)} = y_1$ respectively. We call $GP_{Y_1}(z_1, z_2, y_2)$ the kriging model of y_1 . The DOE on which $GP_{Y_1}(z_1, z_2, y_2)$

is conditioned counts 7 points obtained by Latin Hypercube Sampling (LHS). The second model is approximated by a kriging model called $GP_{Y_2}(z_1, z_2, y_1)$, conditioned on a DOE of 5 points also constructed by a LHS. The parameters of the kriging model are determined by maximum likelihood (see [27]). Note that only 5 and 7 DOE points were used here since the models of Eqn. (14) are relatively simple (linear and quadratic). Furthermore we intentionally limited the number of DOE points in order to be representative of problems involving very expensive simulations where an adaptive construction of the DOE is the most appropriate. Note that our proposed approach would allow such an adaptive selection of a new DOE point in order to reduce the uncertainty on the solution of the MDA problem.

As previously, design variables are set to $z_1 = 6$ and $z_2 = 2$. Figure 3 i) presents the mean of the two kriging models ($GP_{Y_1}(6, 2, y_2)$ and $GP_{Y_2}(6, 2, y_1)$) and the 99% confidence interval (the mean ± 3 standard deviation). A realization of each GP is also drawn on Fig. 3 i) (denoted by random realization).

The approach developed in section 3.2 is now applied. First of all, the KL decomposition of the two conditioned GP is constructed. For both models, the three largest eigenvalues are retained (this choice leads to a variance relative error less than 1% over the studied design space, for both models). Then, the stochastic dimension of the problem is $M = 6$. As mentioned in section 3.3, a simplified version of this problem is also studied in which the covariance of the kriging models is replaced by the assumption of perfect correlation. Then, in this simplified version, the stochastic dimension of the problem is only $n = 2$. Reference results are carried out by MCS of $N_{MCS} = 100000$ simulations. Over these simulations the mean number of iterations to reach convergence is $\mu_{MCS} = 4.58$ with a coefficient of variation of 18%. This approximately leads to 458000 evaluations of each disciplinary solver. The Fig. 3 ii) presents the reference joint PDF of (Y_1, Y_2) .

Table 2 gives the selected PCE degree, the size of the basis and the number of quadrature points used for both approaches. It also presents a comparison of the results obtained by both approaches in terms of number of iterations of Algo. 1, number of disciplinary solver evaluations and values of the error defined by Eqn. (13) for the approximation of the joint CDF of the random vector (Y_1, Y_2) . For computation of this criterion the domain $[5, 35] \times [5, 20]$ is discretized over a 50×50 regular grid. After the selection of points such that $\hat{F}_{MCS}(y^{(i)}) \in [0.01, 0.99]$ one gets $N_{grid} = 1979$.

Finally, Fig. 3 presents the PDF of \hat{Y}_1, \hat{Y}_2 obtained by the *kriging* case, Fig. 3 iii), and by the *simplified kriging* case, Fig. 3 iv). Results presented by Tab. 2 and by Fig. 3 iii) and iv) show that the *kriging* case and the *simplified kriging* case both lead to a good approximation of the reference PDF (Fig. 3 ii)). Moreover, the *simplified kriging* case required approximately 300 times less disciplinary solver evaluations than the *kriging* case to reach a comparable accuracy (CDF mean relative error less than 1%).

From our numerical experiments with this *simplified kriging* case we observed that this simplified version is a cor-

rect approximation of the *kriging* case if there is no DOE point *near* the mean of Y_i , $i = 1, \dots, n$. Definition of a specific criterion must be seen as a prospect of our work, at this time we simply propose an illustration based on the previous example and some qualitative comments at the end of this section.

To illustrate this, a new point is added to the DOE of GP_{Y_1} at coordinates $z_1 = 6, z_2 = 2, y_2 = 13$. The reference PDF of (Y_1, Y_2) is obtained by MCS (100000 simulations) and presented in the Fig. 4 i). The PDF of \hat{Y}_1, \hat{Y}_2 computed with the *kriging* case and with the *simplified kriging* case are respectively given by Fig. 4 ii) and iii). We specify that the parameters of the proposed method (degree, number of quadrature points) remain the same as for the previous example. The error criterion proposed in Eqn. (13) is evaluated on the domain $[32, 42] \times [5, 20]$ discretized on a 100×50 regular grid. After the selection of points such that $\hat{F}_{MCS}(y^{(i)}) \in [0.01, 0.99]$ one gets $N_{grid} = 2991$. Numerical application leads to $Err_{Kg} \approx 1.28\%$ for the *kriging* case and to $Err_{Sim-Kg} \approx 3.53\%$ for the *simplified kriging* case. This confirms the results of Fig. 4 showing that, on this example, the *simplified kriging* case could no longer be considered as good as the *kriging* case. Let us add that the approximation obtained with the *kriging* case is still very efficient.

Two hypotheses are formulated to explain this behavior. First one relies on the fact that, on the vicinity of a DOE point, the correlation of the conditioned Gaussian process tends to zero. Then, the hypothesis of perfect correlation is not correct anymore at the neighborhood of a DOE point. To check this hypothesis we perform a MCS with the perfect correlation assumption. Results (not shown) are almost identical to the one of MCS using the kriging correlation function. Indeed, after a numerical study of the conditioned correlation function, we note that, in this example, the size of the neighborhood in which the perfect correlation assumption is not valid is negligible. Note that this behavior is expected when one deals with kriging interpolation of smooth functions, which is the context of our study. Our second hypothesis is that the polynomial approximations of the responses in a two dimensional space are not able to catch the singularity at a DOE point. Indeed, this hypothesis is confirmed by the improvement of the results by increasing the degree of the PCE (not shown). In practice we increasing the degree to $d = 20$, which allows to get a correct approximation except in the vicinity of the singularity. In order to tackle this issue, a perspective of our research is to try the multi-elements PCE ([21]) on this example as this method is especially devoted to singularity.

4.3 Conceptual aircraft design

4.3.1 Regression models

We consider here the conceptual aircraft design problem described in [31], which was proposed by Airbus as a test case for the Integrative Design for Complex Systems research project. The MDO problem involves determining the engine thrust and the wing area of an aircraft that minimizes, within operational constraints, the maximum take off

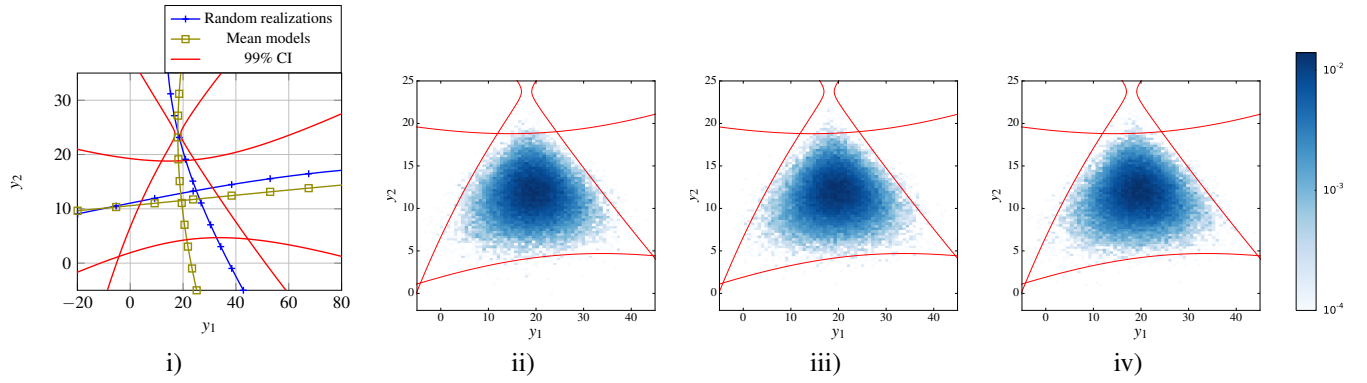


Fig. 3. i) Illustration of the Sellar test case with kriging metamodels, ii) PDF of (Y_1, Y_2) , MCS results (100000 simulations) iii) PDF of \hat{Y}_1, \hat{Y}_2 obtained by PCE *Kriging* case iv) *Simplified kriging* case

Table 2. Comparison between the *kriging* case and the *simplified kriging* case on the Sellar problem. P is the size of the polynomial basis and Q the number of quadrature points.

	degree	Stoc. dim.	P	Q	N_{iter}	Algo. 1	$N_{eval} f_i$	Err
<i>Kriging</i>	3	$M = 6$	84	4096	9		36864	0.673%
<i>Simplified kriging</i>	3	$n = 2$	10	16	7		112	0.846%

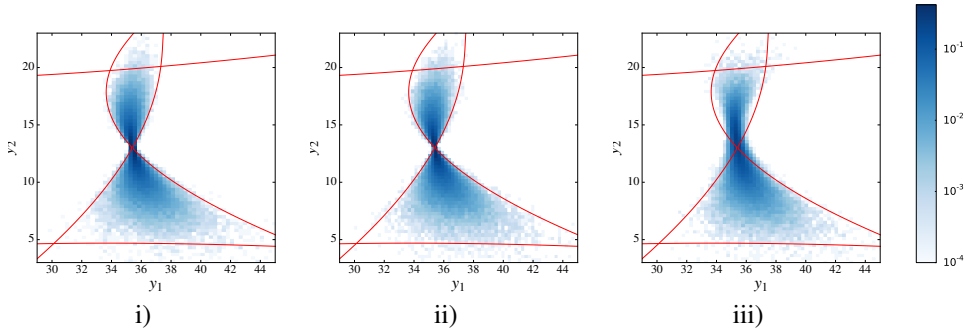


Fig. 4. i) *Kriging* case with a supplementary DOE point for GP_{Y_1} , PDF of (Y_1, Y_2) , MCS results (100000 simulations) ii) PDF of \hat{Y}_1, \hat{Y}_2 obtained by PCE, *Kriging* case iii) *Simplified kriging* case

weight ($mtow$), under a given set of design assumptions and under given regression models based on historical databases. The various models considered involve overall 160 parameters but most of them are fixed (performance requirements or design assumptions) or related through the regression models. The multidisciplinary analysis involves a single feedback loop between the structural and the design mission disciplinary solvers. The design mission solver uses the Breguet Leduc range equation [32] to output the $mtow$ of the aircraft as a function of the zero fuel weight (zfw) of the aircraft and for fixed values of the range (r), the mach number (m), the specific fuel consumption (sfc) and the lift over drag ratio (l/d). Conversely the structural solver provides the zero fuel weight of the aircraft for a given take-off weight, based on structural strength considerations. For the test case, a semi analytic model developed at Onera [33] is used. This model takes the following inputs: the wing surface (w_s), the sweep angle (β), the length of the fuselage (l_f), the diameter of the fuselage (d_f) and the number of passengers n_{pax} . According to our notations, the coupling variables

are $y_1 = mtow$ and $y_2 = zfw$ and the design variables are $z = \{r, m, sfc, l/d, \beta, l_f, d_f, n_{pax}\}$.

It is assumed that both models have been computed from different designs representing a database of existing aircraft. Then, Figure 5 presents the points from the database as well as the corresponding linear regressions with their 99% confidence interval constructed by the method proposed in [31]. This method leads to the definition of the modeling error as a perfectly correlated Gaussian random field. The stochastic dimension of the problem is thus $n = 2$. It should be noted that there is no closed form expression of the variance with respect to the coupling variable contrary to the previous example, hence the variance should be computed pointwise.

As for the previous examples, reference results are obtained with MCS of 100000 simulations. Over these 100000 simulation the mean number of fixed point iterations used to reach the convergence is $\mu_{MC} \approx 27.24$ with a coefficient of variation of 20%. The number of disciplinary solver evaluations is then approximately equal to 2724000.

The PCE approximation for the *perfectly correlated* case

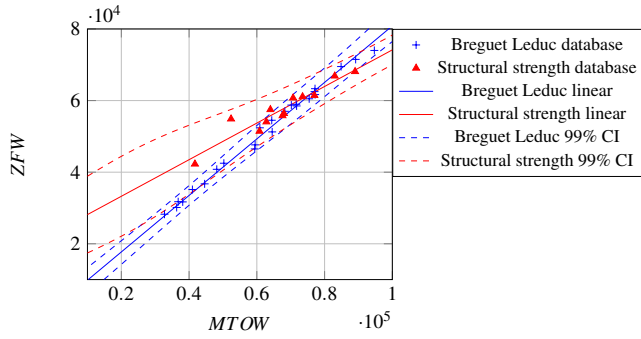


Fig. 5. Illustration of the regression approach based on databases. Linear regressions and 99% CI constructed by the method proposed in [31].

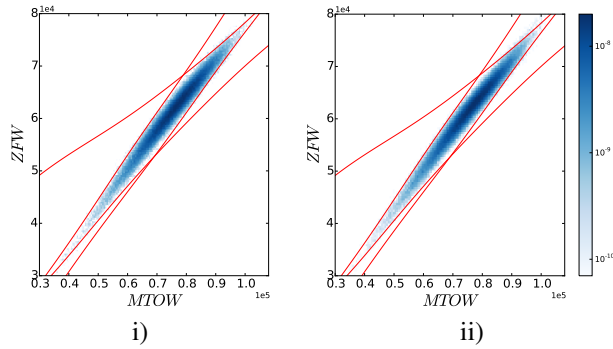


Fig. 6. i) PDF of $(MTOW, ZFW)$ obtained by MCS (100000 simulations) ii) PDF of $MT\hat{O}W, Z\hat{F}W$ obtained by the proposed approach

is set up with a maximal degree $d = 3$, thus the polynomial basis size is $P = 10$. Quadrature level is set to 6, so the number of quadrature points is $Q = 36$. The number of iterations is $N_{iter} \text{ Algo.1} = 57$, hence the number of disciplinary solver evaluations is $N_{eval} f_i = 2052$. Figure 6 i) and ii) respectively present the PDF of $(MTOW, ZFW)$ and the PDF of its PCE approximation $MT\hat{O}W, Z\hat{F}W$. Error criterion defined by Eqn. (13) is evaluated on a regular grid over the domain $[30000, 108000] \times [30000, 80000]$ of size 200×200 . After the selection of points such that $\hat{F}_{MCS}(y^{(i)}) \in [0.01, 0.99]$ one gets $N_{grid} = 18726$, leading to $Err^{(MTOW, ZFW)} = 1.82\%$

This result and the visual comparison presented by Fig. 6 show that the proposed method leads to a correct approximation of the reference probability distribution of the random vector $(MTOW, ZFW)$ for 2052 disciplinary solver evaluations (the mean relative error on the CDF being of approximately 2%). Nevertheless, it is interesting to note that the number of iterations of Algo. 1 is approximately ten times higher than the one obtained on the previous example with the same stochastic dimension $n = 2$. This result illustrates the difficulties encountered by a fixed point algorithm to converge as the residual decreases slowly (in this example this is due to the fact that the two linear relations have very close slopes). This remark can motivate some effort for the

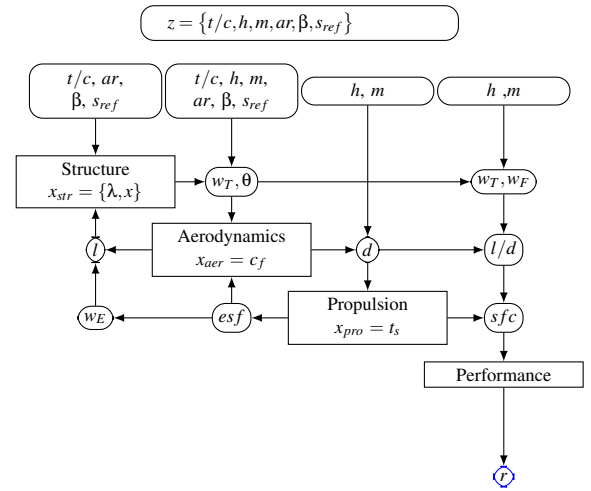


Fig. 7. Conception diagram of the SSBJ test case

Table 3. Values of the design variables used for the SSBJ test case

variable	designation	value
thickness/chord ratio	t/c	0.05
altitude	h	45000 <i>ft</i>
Mach number	m	1.6
Aspect ratio	ar	5.5
Wing sweep	β	55 <i>deg</i>
Wing surface area	s_{ref}	1000 <i>ft</i> ²
Wing taper ratio	λ	0.25
Wingbox x sectional area	x	1
Coefficient of friction	c_f	1
Throttle setting	t_s	0.5

implementation of other nonlinear solvers such as Newton Raphson for solving Eqn. (9). It should also be noted that the same behavior is encountered for MCS as it relies on the same fixed point algorithm.

4.3.2 Supersonic business jet Presentation

This test case has been proposed in [34] for the evaluation of the BLISS MDO architecture and it is a common test case in the MDO community. Objective is to maximize the range of a supersonic business jet (SSBJ) with respect to the structural strength, the aerodynamics and the propulsion. Figure 7 presents the SSBJ test case and details the feedback loops between the structural, aerodynamics and propulsion solvers. z denotes the vector of shared design variables, x_{str} , x_{aer} and x_{pro} are the vectors of local design variables. All these variables are set to their initial values (see [34]). Table 3 gives the details of the numerical values and designation of each variables.

This test case counts 6 coupling variables that are the

wing twist θ , the total weight w_T , the lift coefficient l , the drag coefficient d , the engine scale factor esf and the engine weight w_E . These 6 variables are linked by the following nonlinear system

$$\begin{aligned}\theta &= g_1(l, z, x_{str}) \\ w_T &= g_2(l, w_E, z, x_{str}) \\ l &= g_3(w_T) \\ d &= g_4(w_T, \theta, esf, z, x_{aer}) \\ esf &= g_5(d, x_{pro}) \\ w_E &= g_6(d)\end{aligned}\quad (15)$$

The range is then computed by the Breguet Leduc equation,

$$r = \frac{661\sqrt{0.7519}(l/d)m}{sfc} \ln\left(\frac{w_T}{w_T - w_F}\right) \quad (16)$$

where $sfc = g_7(z, x_{pro})$ is the specific fuel consumption and $w_f = g_8(z)$ is the fuel weight. Implementation details of g_k , $k = 1, \dots, 8$ can be found in the annex of [34].

In the following, all disciplinary solvers g_k , $k = 1, \dots, 8$ are approximated by kriging surrogate models. As for the Sellar example, independent DOE per discipline are used to construct the kriging models. Hence, the kriging models of g_1 , g_2 , g_8 respectively called GP_θ , GP_{w_T} , GP_{w_F} are build on the same DOE of 80 points, the kriging models of g_3 , g_4 respectively called GP_L , GP_D are build on a second DOE of 100 points and the kriging models of g_5 , g_6 , g_7 respectively called GP_{ESF} , GP_{w_E} and GP_{SFC} are build on a third DOE of 100 points. These three DOE are constructed by LHS.

Based on our previous comparison on *kriging* and *simplified kriging* and considering the higher stochastic dimension of the problem the *simplified kriging* assumption will be used. The validity of this assumption will be confirmed once the results obtained. The stochastic version of Eqn. (15) thus reads,

$$\begin{aligned}\Theta &= f_1(L, z, x_{str}) + \varepsilon_1(L, z, x_{str}) \\ W_T &= f_2(L, w_E, z, x_{str}) + \varepsilon_2(L, w_E, z, x_{str}) \\ L &= f_3(W_T) + \varepsilon_3(W_T) \\ D &= f_4(W_T, \Theta, ESF, z, x_{aer}) + \varepsilon_4(W_T, \Theta, ESF, z, x_{aer}) \\ ESF &= f_5(D, x_{pro}) + \varepsilon_5(D, x_{pro}) \\ W_E &= f_6(D) + \varepsilon_6(D)\end{aligned}\quad (17)$$

where f_i , $i = 1, \dots, 6$ are the mean prediction of the kriging models and ε_i , $i = 1, \dots, 6$ are zero mean normal random variables with standard deviation given by the kriging models.

Once the PCE approximation of the 6 coupling variables is obtained, a classical PCE approach is used to compute the PCE approximation of the range. To this purpose we consider the two other surrogate models, $SFC = f_7(z, x_{pro}) + \varepsilon_7(z, x_{pro})$ and $W_f = f_8(z) + \varepsilon_8(z)$ where f_7 and f_8 are the mean prediction of the corresponding kriging models and ε_7 and ε_8 are zero mean normal random variables with variance specified by the kriging models.

Finally, this test case is solved in two steps. First by computing the PCE approximation of the 6 coupling variables. This resolution is achieved by the proposed method with the *simplified kriging* assumption. The stochastic dimension of the problem is thus $n = 6$. Then, in a second step, the PCE approximation of the range is computed by classical PCE. This second problem has a stochastic dimension $n = 8$ but without any feedback loop.

Resolution and comparisons

Reference results are obtained by MCS with 100000 simulations. The mean number of fixed point iterations to reach convergence is $\mu_{MC} \approx 11.12$ with a standard deviation of 3%. The number of disciplinary solver evaluations is then approximately 1112000. For the PCE approximation, the degree is set to $d = 3$ leading to a polynomial basis of size $P = 84$ and the quadrature level is set to 3 leading to a number of quadrature nodes $Q = 729$. The number of iterations of Algo. 1 to converge is $N_{iter} = 11$. The number of disciplinary solver iteration is thus equal to $N_{eval} = 8029$.

Figure 8 presents the PDF by pairs between the 6 coupling variables. The lower triangular part presents the MCS reference results and the upper triangular part the results obtained by the proposed method. The diagonal contains two superposed histograms of the marginal PDF, one obtained by MCS and one by the proposed approach. This figure allows to conclude that the PCE approximation catches the global behavior of the joint probability distribution. Indeed, concerning the marginal PDF, the two histograms are almost perfectly superposed, and concerning the pairs PDF, results by MCS and by PCE seem very similar. In order to confirm this visual results, the error criterion defined by Eqn. (13) is computed by pairs on 50×50 grids ad presented in Tab. 4. Note that in parenthesis is given the number of points N_{grid} such that $\hat{F}_{MCS}(y^{(i)}) \in [0.01, 0.99]$. The approximation obtained by the proposed approach leads to a CDF mean relative error less than 1% for all the pairs of variables, which confirms the accuracy of the method.

After these results on the coupled problem solved by Algo. 1, we present some results on the objective function,

$$R = \frac{661\sqrt{0.7519}(L/D)m}{SFC} \ln\left(\frac{W_T}{W_T - W_F}\right)$$

whose PCE, \hat{R} , is computed based on the previous results. The interest of the PCE approximation in terms of obtaining the GSA at no additional cost is illustrated on \hat{R} . The method proposed in [18] is used to compute the first order Sobol' indices [35] denoted by $S_1^{(\varepsilon_i)}$, $i = 1, \dots, 8$. The following results are obtained, $S_1^{(\varepsilon_1)} = 6.56 \times 10^{-4}$, $S_1^{(\varepsilon_2)} = 4.96 \times 10^{-4}$, $S_1^{(\varepsilon_3)} = 7.02 \times 10^{-2}$, $S_1^{(\varepsilon_4)} = 9.11 \times 10^{-1}$, $S_1^{(\varepsilon_5)} = 2.07 \times 10^{-3}$, $S_1^{(\varepsilon_6)} = 5.25 \times 10^{-4}$, $S_1^{(\varepsilon_7)} = 7.50 \times 10^{-6}$ and $S_1^{(\varepsilon_8)} = 1.35 \times 10^{-2}$. As a first comment, one can note that the sum of the first order Sobol' indices is almost equal to 1 (≈ 0.9987) which indicates that there is no interaction between the model uncertainties. Moreover, this indices allows

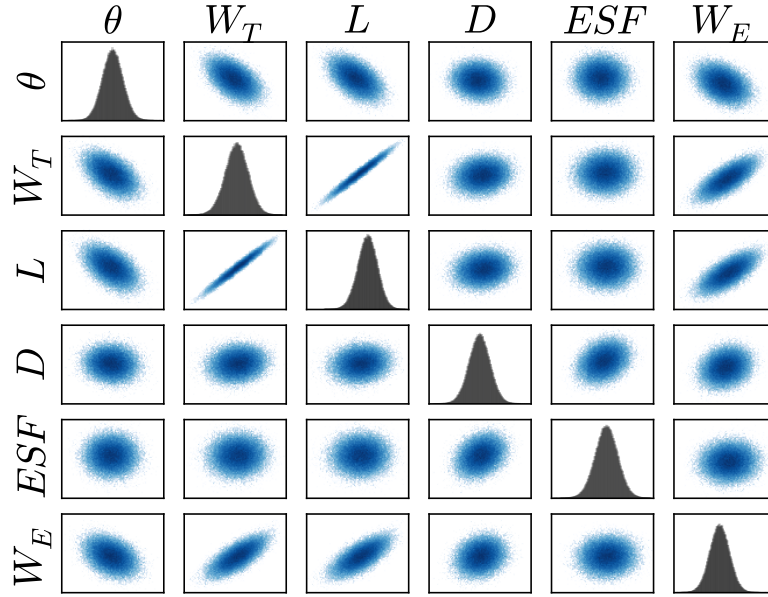


Fig. 8. Comparison between the MCS and the proposed method results. The lower triangular part presents the MCS PDF whereas the upper triangular part presents the PDF obtained with the proposed method. On the diagonal the histograms of the marginal obtained by both methods are superposed.

Table 4. Evaluation of the error criterion defined by Eqn. (13) by pairs of variables for the 6 coupling variables of the SSBJ test case. Between parenthesis is given the number of points of evaluation N_{grid}

Variables	(θ, W_T)	(θ, L)	(θ, D)	(θ, ESF)	(θ, W_E)	(W_T, L)
Err	0.78% (1132)	0.74% (1126)	0.77% (1145)	0.95% (1190)	0.63% (1201)	0.97% (1333)
Variables	(W_T, D)	(W_T, ESF)	(W_T, W_E)	(L, D)	(L, ESF)	(L, W_E)
Err	0.93% (1193)	0.78% (1201)	0.80% (1351)	0.95% (1195)	0.72% (1197)	0.77% (1358)
Variables	(D, ESF)	(D, W_E)	(ESF, W_E)			
Err	0.82% (1183)	0.80% (1238)	0.63% (1251)			

to rank the surrogate models that must be improved in order to decrease the variance of the response R . In this example, the index related to ε_4 clearly dominates the others. Then, according to the notation of Eqn. (17) the surrogate model GP_D , that computes the drag coefficient, must be improved to decrease the variance of the range R .

5 Conclusions

The present paper addresses the problem of modeling uncertainties propagation in a multidisciplinary analysis. It is assumed that uncertainties are modeled by random fields over the design and coupling variables space. Two particular cases are studied namely the *perfectly correlated* case and the *kriging* case. These two cases are retained for their relevance from a practical point of view. Indeed, the first one corresponds to the case where modeling uncertainties are based on expert judgment or historical databases whereas the second case corresponds to the use of kriging surrogate models. Ac-

ording to these hypothesis the random MDA problem consists in solving a random nonlinear system (as presented by section 2.2).

The proposed method is based on the resolution of this nonlinear system by a semi intrusive polynomial chaos expansion approach. The method is denoted by *semi intrusive* as each equation of the random nonlinear system is approximated by a non intrusive PCE (the projection approach is retained) but the solver of the deterministic nonlinear system has to be adapted intrusively (an adaptation of the fixed point algorithm is proposed).

Perspectives of this work include moving from scalar output of the disciplinary solvers to field output. Indeed design of complex multidisciplinary systems (e.g. aerostructural wing design) may involve exchanging vector-fields between disciplines. In order to achieve this challenging problem, coupling the proposed non intrusive PCE approach with model order reduction could be investigated. A second perspective of this work is its application to MDO. The proposed

approach could be particularly beneficial in the context of a noisy, kriging based adaptive optimization framework. Indeed the uncertainty estimation we obtain at a given design point can be used to determine whether to refine or not the models in the context of improving the objective function. Note that while our approach for propagating uncertainty would need to be repeated at each new iteration point of the optimization, we can significantly accelerate the fixed point calculation in Algo. 1 by a smart initial guess for the PCE coefficients (for example the solution at the nearest design point).

Acknowledgements

This work is supported by the European project H2020 AGILE. The support is gratefully acknowledge. The authors would like to thank reviewers for their relevant comments.

References

- [1] Chittick, I. R., and Martins, J. R. R. A., 2008. “An asymmetric suboptimization approach to aerostructural optimization”. *Optimization and Engineering*, **10**(1), pp. 133–152.
- [2] Martins, J. R. R. A., and Lambe, A. B., 2013. “Multidisciplinary Design Optimization: A Survey of Architectures”. *AIAA Journal*, **51**(9), pp. 2049–2075.
- [3] Liang, C., Mahadevan, S., and Sankararaman, S., 2015. “Stochastic Multidisciplinary Analysis Under Epistemic Uncertainty”. *Journal of Mechanical Design*, **137**, p. 021404 12 pages.
- [4] Zang, T., Hemsch, M., Hilburger, M., Kenny, S., Luckring, J., Maghami, P., Padula, S., and Jefferson Stroud, W., 2002. Needs and Opportunities for Uncertainty Based Multidisciplinary Design Methods for Aerospace Vehicles. Tech. Rep. TM-2002-211462, NASA Langley Research Center Rept.
- [5] Jones, D. R., Schonlau, M., and Welch, W. J., 1998. “Efficient global optimization of expensive black-box functions”. *Journal of Global Optimization*, **13**(4), pp. 455–492.
- [6] Brevault, L., Balesdent, M., Bérend, N., and Le Riche, R., 2015. “Decoupled MDO formulation for interdisciplinary coupling satisfaction under uncertainty”. *AIAA Journal*, pp. In Press, Accepted Manuscript.
- [7] Sankararaman, S., and Mahadevan, S., 2012. “Likelihood-Based Approach to Multidisciplinary Analysis Under Uncertainty”. *Journal of Mechanical Design*, **134**(3), p. 031008 12 pages.
- [8] Leotardi, C., Diez, M., Serani, A., Iemma, U., and Fortunato Campana, E., 2014. “A Framework for Efficient Simulation-Based Multidisciplinary Robust Design Optimization with Application to a Keel Fin of a Racing Sailboat”. In An International Conference on Engineering and Applied Sciences optimization (OPTI2014), edited by Papadrakakis M. and Karlaftis M.G. and Lagaros N.D.
- [9] Koch, P., Wujek, B., Golovidov, O., and Simpson, T., 2002. “Facilitating Probabilistic Multidisciplinary Design Optimization Using Kriging Approximation Models”. In 9th AIAA/ISSMO Symposium on Multidisciplinary Analysis and Optimization, AIAA Paper 2002-5415.
- [10] Oakley, D. R., Sues, R. H., and Rhodes, G. S., 1998. “Performance optimization of multidisciplinary mechanical systems subject to uncertainties”. *Probabilistic Engineering Mechanics*, **13**(1), pp. 15 – 26.
- [11] Forrester, A., Sobester, A., and Keane, A., 2008. *Engineering design via surrogate modelling: a practical guide*. John Wiley & Sons.
- [12] Jaulin, L., 2001. *Applied interval analysis: with examples in parameter and state estimation, robust control and robotics*, Vol. 1. Springer Science & Business Media.
- [13] Zadeh, L. A., 1965. “Fuzzy sets”. *Information and control*, **8**(3), pp. 338–353.
- [14] Shafer, G., et al., 1976. *A mathematical theory of evidence*, Vol. 1. Princeton university press Princeton.
- [15] Dubois, D., and Prade, H., 2012. *Possibility theory: an approach to computerized processing of uncertainty*. Springer Science & Business Media.
- [16] Ferson, S., Joslyn, C. A., Helton, J. C., Oberkampf, W. L., and Sentz, K., 2004. “Summary from the epistemic uncertainty workshop: consensus amid diversity”. *Reliability Engineering & System Safety*, **85**(1), pp. 355–369.
- [17] Roy, C. J., and Oberkampf, W. L., 2011. “A comprehensive framework for verification, validation, and uncertainty quantification in scientific computing”. *Computer Methods in Applied Mechanics and Engineering*, **200**(25-28), pp. 2131 – 2144.
- [18] Sudret, B., 2008. “Global sensitivity analysis using polynomial chaos expansions”. *Reliability Engineering & System Safety*, **93**(7), pp. 964 – 979. Bayesian Networks in Dependability.
- [19] Ghanem, R. G., and Spanos, P. D., 1991. *Stochastic finite elements: a spectral approach*. Springer, New York, NY.
- [20] Soize, C., and Ghanem, R., 2004. “Physical systems with random uncertainties: Chaos representations with arbitrary probability measure”. *SIAM Journal on Scientific Computing*, **26**(2), pp. 395–410.
- [21] Xiu, D., and Karniadakis, G. E., 2002. “The Wiener-Askey Polynomial Chaos for Stochastic Differential Equations”. *SIAM J. Sci. Comput.*, **24**(2), Feb., pp. 619–644.
- [22] Poëtte, G., and Lucor, D., 2012. “Non intrusive iterative stochastic spectral representation with application to compressible gas dynamics”. *Journal of Computational Physics*, **231**(9), pp. 3587 – 3609.
- [23] Wan, X., and Karniadakis, G. E., 2005. “An adaptive multi-element generalized polynomial chaos method for stochastic differential equations”. *Journal of Computational Physics*, **209**(2), pp. 617 – 642.
- [24] Lebrun, R., and Dutfoy, A., 2009. “A generalization of the nataf transformation to distributions with elliptical copula”. *Probabilistic Engineering Mechanics*, **24**(2), pp. 172 – 178.
- [25] Lebrun, R., and Dutfoy, A., 2009. “Do Rosenblatt and Nataf isoprobabilistic transformations really differ?”. *Probabilistic Engineering Mechanics*, **24**(4), pp. 577 – 584.
- [26] Krige, D. G., 1951. “A statistical approach to some mine evaluations and allied problems at the witwatersrand”. Master’s thesis, University of Witwatersrand.
- [27] Rasmussen, C. E., and Williams, C. K. I., 2006. *Gaussian processes for machine learning*. Adaptive computation and machine learning. MIT Press, Cambridge, Mass.
- [28] Pedregosa, F., Varoquaux, G., Gramfort, A., Michel, V., Thirion, B., Grisel, O., Blondel, M., Prettenhofer, P., Weiss, R., Dubourg, V., Vanderplas, J., Passos, A., Cournapeau, D., Brucher, M., Perrot, M., and Duchesnay, E., 2011. “Scikit-learn: Machine learning in Python”. *Journal of Machine Learning Research*, **12**, pp. 2825–2830.

- [29] Sellar, R. S., Batill, S. M., and Renaud, J. E., 1996. "Response surface based, concurrent subspace optimization for multidisciplinary system design". In 34th AIAA Aerospace Sciences Meeting and Exhibit, pp. 96–0714.
- [30] Shizgal, B. D., and Jung, J.-H., 2003. "Towards the resolution of the Gibbs phenomena ". *Journal of Computational and Applied Mathematics* , **161**(1), pp. 41 – 65.
- [31] Jaeger, L., Gogu, C., Segonds, S., and Bes, C., 2013. "Aircraft Multidisciplinary Design Optimization Under Both Model and Design Variables Uncertainty". *Journal of Aircraft*, **50**(2), Feb., pp. 528–538.
- [32] Ruijgrok, G., 1990. *Elements of Airplane Performance*. Delft University Press.
- [33] Lefebvre, T., Schmollgruber, P., Blondeau, C., and Carrier, G., 2012. "Aircraft conceptual design in a multi-level, multi-fidelity, multi-disciplinary optimization process". In 28th ICAS congress, Brisbane (Australia).
- [34] Sobieszczanski, J., Agte, J., and Sandusky, R., 1998. Bi-level integrated system synthesis (bliss). Tech. rep.
- [35] Sobol, I. M., 2001. "Global sensitivity indices for nonlinear mathematical models and their Monte Carlo estimates". *Mathematics and computers in simulation*, **55**(1), pp. 271–280.